

Concerning the quark condensate

K. Langfeld,¹ H. Markum,² R. Pullirsch,³ C. D. Roberts,^{4,5} and S. M. Schmidt^{1,6}

¹*Institut für Theoretische Physik, Universität Tübingen, Auf der Morgenstelle 14, D-72076 Tübingen, Germany*

²*Atominstytut, Technische Universität Wien, A-1040 Vienna, Austria*

³*Institut für Theoretische Physik, Universität Regensburg, D-93040 Regensburg, Germany*

⁴*Physics Division, Building 203, Argonne National Laboratory, Argonne, Illinois 60439-4843, USA*

⁵*Fachbereich Physik, Universität Rostock, D-18051 Rostock, Germany*

⁶*Helmholtz-Gemeinschaft, Ahrstrasse 45, D-53175 Bonn, Germany*

(Received 8 January 2003; published 30 June 2003)

A continuum expression for the trace of the massive dressed-quark propagator is used to explicate a connection between the infrared limit of the QCD Dirac operator's spectrum and the quark condensate appearing in the operator product expansion. This connection is verified via comparison with a lattice-QCD simulation. The pseudoscalar vacuum polarization provides a good approximation to the condensate over a larger range of current-quark masses.

DOI: 10.1103/PhysRevC.67.065206

PACS number(s): 12.38.Aw, 11.30.Qc, 11.30.Rd, 24.85.+p

I. INTRODUCTION

Dynamical chiral symmetry breaking (DCSB) is a cornerstone of hadron physics. This phenomenon whereby, even in the absence of a current-quark mass, self-interactions generate a momentum-dependent running quark mass $M(p^2)$ that is large in the infrared, $M(0) \sim 0.5$ GeV, but, in the chiral limit, power-law suppressed in the ultraviolet [1],

$$M(p^2) \stackrel{\text{large-}p^2}{=} \frac{\text{large-}p^2 2\pi^2 \gamma_m}{3} \frac{(-\langle \bar{q}q \rangle^0)}{p^2 \left(\frac{1}{2} \ln \left[\frac{p^2}{\Lambda_{\text{QCD}}^2} \right] \right)^{1-\gamma_m}}, \quad (1)$$

is impossible in weakly interacting theories. In Eq. (1), $\gamma_m = 12/(33 - 2N_f)$ is the mass anomalous dimension, with N_f the number of light-quark flavors, and $\langle \bar{q}q \rangle^0$ is the renormalization-group-invariant vacuum quark condensate [2], to which we shall hereafter refer as the OPE condensate. While Eq. (1) is expressed in Landau gauge, $\langle \bar{q}q \rangle^0$ is gauge parameter independent. In the chiral limit the OPE condensate plays a role analogous to that played by the renormalization-group-invariant current-quark mass in the massive theory: it sets the scale of the mass function in the ultraviolet.

The evolution of the dressed-quark mass function in Eq. (1) to a large and finite constituent-quark-like mass in the infrared, $M(0) \sim 0.5$ GeV, is a longstanding prediction of Dyson-Schwinger equation (DSE) studies [3], which has recently been confirmed in simulations of quenched lattice-QCD [4]. A determination of the OPE condensate directly from lattice-QCD simulations must await an accurate chiral extrapolation [5], but DSE models tuned to reproduce modern lattice data give [6] $(-\langle \bar{q}q \rangle^0) \sim \Lambda_{\text{QCD}}^3$.

Another view of DCSB is obtained by considering the eigenvalues and eigenfunctions of the massless Euclidean Dirac operator [7],

$$\gamma \cdot D u_n(x) = i \lambda_n u_n(x). \quad (2)$$

The operator is anti-Hermitian and hence the eigenfunctions form a complete set, and except for zero modes they occur in pairs: $\{u_n(x), \gamma_5 u_n(x)\}$, with eigenvalues of opposite sign. It follows that in an external gauge field A , one can write the Green function for a massive propagating quark in the form

$$S(x, y; A) = \langle q(x) \bar{q}(y) \rangle_A = \sum_n \frac{u_n(x) u_n^\dagger(y)}{i \lambda_n + m}, \quad (3)$$

where m is the current-quark mass and, naturally, the eigenvalues depend on A . [The expectation value denotes a Grassmannian functional integral evaluated with a fixed gauge field configuration. This equation merely expresses the resolvent of the Dirac operator in terms of the complete set of eigenfunctions in Eq. (2).] Taking the matrix trace in Eq. (3) and the limit $y \rightarrow x$, and assuming, e.g., a lattice regularization, one obtains

$$\frac{1}{V} \int_V d^4x \langle \bar{q}(x) q(x) \rangle_A = - \frac{2m}{V} \sum_{\lambda_n > 0} \frac{1}{\lambda_n^2 + m^2}, \quad (4)$$

where V is the lattice volume and here m is the current-quark mass at the lattice regularization scale [8].

One may now define a quark condensate as the infinite volume limit of the average of the left-hand side in Eq. (4) over all gauge field configurations,

$$\langle 0 | \bar{q}q | 0 \rangle := \lim_{V \rightarrow \infty} \left\langle \frac{1}{V} \int_V d^4x \langle \bar{q}(x) q(x) \rangle_A \right\rangle. \quad (5)$$

In the limit $V \rightarrow \infty$, the operator spectrum becomes dense and Eqs. (4) and (5) yield

$$-\langle 0 | \bar{q}q | 0 \rangle = 2m \int_0^\infty d\lambda \frac{\rho(\lambda)}{\lambda^2 + m^2}, \quad (6)$$

with $\rho(\lambda)$ the spectral density. This equation expresses an assumption that in QCD the full two-point massive-quark

Schwinger function, when viewed as a function of the current-quark mass, has a spectral representation. It follows formally from Eq. (6) that

$$\lim_{m \rightarrow 0} m \int_0^\infty d\lambda \frac{\rho(\lambda)}{\lambda^2 + m^2} = \frac{1}{2} \pi \rho(0), \quad (7)$$

and hence one arrives at the chiral limit result

$$-\langle 0 | \bar{q} q | 0 \rangle = \pi \rho(0). \quad (8)$$

This is the so-called Banks-Casher relation [10,11]. (The discussion hitherto is a motivation, not a derivation: rigorous understanding is provided in Ref. [9] and subsequently herein.)

The Banks-Casher relation has long been advocated as a means by which a quark condensate may be measured in lattice-QCD simulations [11]. It has also been used in analyzing chiral symmetry restoration at nonzero temperature [12] and chemical potential [13], and to explore the connection between magnetic monopoles and chiral symmetry breaking in U(1) gauge theory [14]. Much has been learnt [15,16] by exploiting the fact that qualitative features of the behavior of $\rho(\lambda)$ for $\lambda \sim 0$ can be understood using chiral random matrix theory; i.e., from considerations based solely on QCD's global symmetries.

Our main goal is to explicate a correspondence between the condensate in Eq. (1) and that in Eq. (8). In Sec. II we discuss the OPE condensate and its connection with QCD's gap equation, and emphasize that the residue of the lowest-mass pole contribution to the flavor-nonsinglet pseudoscalar vacuum polarization is a direct measure of the OPE condensate [17]. A natural ability to express DCSB through the formation of a nonzero OPE condensate is fundamental to the success of DSE models of hadron phenomena [18]. In Sec. III we carefully define the trace of the massive dressed-quark propagator and use that to illustrate a connection between $\rho(0)$ and the OPE condensate, which we verify via comparison with a lattice simulation. Section IV is an epilogue.

II. OPE CONDENSATE

A. Gap and Bethe-Salpeter equations

Dynamical chiral symmetry breaking in QCD is readily explored using the DSE for the quark self-energy:

$$S(p)^{-1} = Z_2(i\gamma \cdot p + m^{\text{bm}}) + Z_1 \int_q^\Lambda g^2 D_{\mu\nu}(p-q) \times \frac{\lambda^a}{2} \gamma_\mu S(q) \Gamma_\nu^a(q,p), \quad (9)$$

where $D_{\mu\nu}(k)$ is the renormalized dressed-gluon propagator; $\Gamma_\nu^a(q,p)$ is the renormalized dressed-quark-gluon vertex; m^{bm} is the Λ -dependent current-quark bare mass that appears in the Lagrangian; and $\int_q^\Lambda := \int^\Lambda d^4q / (2\pi)^4$ represents a translationally invariant regularization of the integral, with Λ the regularization mass scale that is removed to infinity as the

completion of all calculations. The quark-gluon vertex and quark wave function renormalization constants, $Z_1(\xi^2, \Lambda^2)$ and $Z_2(\xi^2, \Lambda^2)$ respectively, depend on the renormalization point, the regularization mass scale, and the gauge parameter.

If the current-quark mass changes with flavor, then the solution of Eq. (9) is flavor dependent:

$$S_f(p)^{-1} = i\gamma \cdot p A_f(p^2, \xi^2) + B_f(p^2, \xi^2) = \frac{1}{Z_f(p^2, \xi^2)} [i\gamma \cdot p + M_f(p^2, \xi^2)], \quad (10)$$

and is obtained subject to the condition that at some large, spacelike ξ^2 ,

$$S_f(p)^{-1} \Big|_{p^2 = \xi^2} = i\gamma \cdot p + m_f(\xi), \quad (11)$$

where $m_f(\xi)$ is the renormalized current-quark mass,

$$Z_4(\xi, \Lambda) m_f(\xi) = Z_2(\xi, \Lambda) m_f^{\text{bm}}(\Lambda), \quad (12)$$

with Z_4 the renormalization constant for the scalar part of the quark self-energy. Since QCD is an asymptotically free theory, the chiral limit is defined by

$$Z_2(\xi^2, \Lambda^2) m_f^{\text{bm}}(\Lambda) \equiv 0, \quad \Lambda \gg \xi \quad (13)$$

and in this case the scalar projection of Eq. (9) does not exhibit an ultraviolet divergence [2,17].

Important in describing chiral symmetry is the axial-vector Ward-Takahashi identity:

$$P_\mu \Gamma_{5\mu}^H(k; P) = \mathcal{S}^{-1}(k_+) i\gamma_5 \frac{T^H}{2} + i\gamma_5 \frac{T^H}{2} \mathcal{S}^{-1}(k_-) - M_{(\zeta)} i\Gamma_5^H(k; P) - i\Gamma_5^H(k; P) M_{(\zeta)}, \quad (14)$$

where P is the total momentum entering the vertex. In Eq. (14), $M_{(\zeta)} = \text{diag}[m_u(\zeta), m_d(\zeta), m_s(\zeta)]$, $\mathcal{S} = \text{diag}[S_u, S_d, S_s]$, and $\{T^H\}$ are flavor matrices, e.g., $T^{\pi^+} = \frac{1}{2}(\lambda^1 + i\lambda^2)$ [we consider $\text{SU}_f(3)$ because chiral symmetry is unimportant for heavier quarks]; $\Gamma_{5\mu}^H(k; P)$ is the renormalized axial-vector vertex, which is obtained from the inhomogeneous Bethe-Salpeter equation

$$[\Gamma_{5\mu}^H(k; P)]_{tu} = Z_2 \left[\gamma_5 \gamma_\mu \frac{T^H}{2} \right]_{tu} + \int_q^\Lambda [\chi_{5\mu}^H(q; P)]_{sr} K_{tu}^{rs}(q, k; P), \quad (15)$$

where $\chi_{5\mu}^H := \mathcal{S}(q_+) \Gamma_{5\mu}^H(q; P) \mathcal{S}(q_-)$, $q_\pm = q \pm P/2$, and $K(q, k; P)$ is the fully renormalized quark-antiquark scattering kernel; and Γ_5^H is the pseudoscalar vertex,

$$[\Gamma_5^H(k; P)]_{tu} = Z_4 \left[\gamma_5 \frac{T^H}{2} \right]_{tu} + \int_q^\Lambda [\chi_5^H(q; P)]_{sr} K_{tu}^{rs}(q, k; P), \quad (16)$$

with $\chi_5^H := \mathcal{S}(q_+) \Gamma_5^H(q; P) \mathcal{S}(q_-)$. Multiplicative renormalizability ensures that no new renormalization constants appear in Eqs. (15) and (16).

Flavor-octet pseudoscalar bound states appear as coincident pole solutions of Eqs. (15) and (16), namely,

$$\Gamma_{5\mu}^H(k; P) \propto \Gamma_5^H(k; P) \propto \frac{1}{P^2 + m_H^2} \Gamma_H(k; P), \quad (17)$$

where Γ_H is the bound state's Bethe-Salpeter amplitude and m_H its mass. (Regular terms are overwhelmed at the pole.) Consequently, Eq. (14) entails [2,17]

$$f_H m_H^2 = r_H^{(\zeta)} \mathcal{M}_H^{(\zeta)}, \quad (18)$$

where $\mathcal{M}_H^{(\zeta)} = \text{tr}_{\text{flavor}} [M_{(\zeta)} \{T^H, (T^H)^\dagger\}]$ is the sum of the constituents' current-quark masses ("t" denotes matrix transpose); and

$$f_H P_\mu = Z_2 \int_q^{\Lambda 1} \frac{1}{2} \text{tr}[(T^H)^\dagger \gamma_5 \gamma_\mu \chi_H(q; P)], \quad (19)$$

$$i r_H^{(\zeta)} = Z_4 \int_q^{\Lambda 1} \frac{1}{2} \text{tr}[(T^H)^\dagger \gamma_5 \chi_H(q; P)], \quad (20)$$

where $\chi_H := \mathcal{S}(q_+) \Gamma_H(q; P) \mathcal{S}(q_-)$ and the expressions are evaluated at $P^2 + m_H^2 = 0$.

Equation (19) is the pseudovector projection of the meson's Bethe-Salpeter wave function evaluated at the origin in configuration space. It is the precise expression for the leptonic decay constant. The renormalization constant $Z_2(\zeta, \Lambda)$ ensures that the right-hand side (rhs) is independent of: the regularization scale Λ , which may therefore be removed to infinity; the renormalization point; and the gauge parameter. Hence it is truly an observable.

Equation (20) is the pseudoscalar analog. Therein the renormalization constant $Z_4(\zeta, \Lambda)$ entails that the rhs is independent of the regularization scale Λ and the gauge parameter. It also ensures that the ζ dependence of $r_H^{(\zeta)}$ is precisely that required to guarantee that the rhs of Eq. (18) is independent of the renormalization point. [$r_H^{(\zeta)}$ is finite, and Eq. (18) valid, for arbitrary values of the current-quark masses [19,20].]

In the chiral limit the existence of a solution of Eq. (9) with $B_0(p^2) \neq 0$; i.e., DCSB, necessarily entails [17] that Eqs. (15) and (16) exhibit a massless pole solution: the Goldstone mode, which is described by

$$\begin{aligned} \Gamma_0^g(k; P) = & \lambda^g \gamma_5 [i E_0(k; P) + \gamma \cdot P F_0(k; P) \\ & + \gamma \cdot k k \cdot P G_0(k; P) + \sigma_{\mu\nu} k_\mu P_\nu H_0(k; P)], \end{aligned} \quad (21)$$

wherein $f_\pi^0 E_0(k; 0) = B_0(k^2)$. (The index "0" indicates a quantity calculated in the chiral limit.) It follows immediately [17] that

$$f_\pi^0 r_0^{(\zeta)} = -\langle \bar{q} q \rangle_\zeta^0 = \lim_{\Lambda \rightarrow \infty} Z_4(\zeta, \Lambda) N_c \text{tr}_D \int_q^\Lambda S_0(q), \quad (22)$$

where the trace is only over Dirac indices. This result and multiplicative renormalizability entail

$$\frac{\langle \bar{q} q \rangle_\zeta^0}{\langle \bar{q} q \rangle_{\zeta'}^0} = Z_4(\zeta, \zeta') Z_2^{-1}(\zeta, \zeta') = Z_m(\zeta, \zeta'), \quad (23)$$

where Z_m is the mass-renormalization constant. It is thus apparent that the chiral limit behavior of $r_H^{(\zeta)}$ yields the OPE condensate evolved to a renormalization point ζ .

It is important to recall that the DSEs reproduce every diagram in perturbation theory. Therefore a weak coupling expansion of Eq. (9) yields the perturbative series for the dressed-quark propagator. This may be illustrated by the result for the scalar piece of the propagator calculated in this way,

$$B_f(p^2) = m_f \left(1 - \frac{\alpha}{\pi} \ln \left[\frac{p^2}{m_f^2} \right] + \dots \right). \quad (24)$$

Every term in the series is proportional to the current-quark mass and hence a nonzero value of the OPE condensate is impossible in perturbation theory.

B. Pseudoscalar vacuum polarization

Consider the color singlet Schwinger function describing the pseudoscalar vacuum polarization

$$\Delta_5(x) = \left\langle \bar{q}(x) \frac{1}{2} \lambda^f \gamma_5 q(x) \bar{q}(0) \frac{1}{2} \lambda^g \gamma_5 q(0) \right\rangle, \quad (25)$$

which can be estimated, e.g., in lattice simulations. Its renormalized form can completely be expressed in momentum space using quantities introduced already,

$$\omega_5^{fg}(P) = Z_2^2 \text{tr} \int_q^{\Lambda 1} \frac{1}{2} \lambda^f \gamma_5 \mathcal{S}(q_+) \Gamma_5^g(q; P) \mathcal{S}(q_-). \quad (26)$$

Equation (16) can be rewritten in terms of the fully amputated quark-antiquark scattering amplitude: $M = K + K(SS)K + \dots$, and in the neighborhood of the lowest mass pole

$$M(q, k; P) = \Gamma_H(q; P) \frac{1}{P^2 + m_H^2} \bar{\Gamma}(k; -P) + R(q, k; P), \quad (27)$$

where R is regular in this neighborhood.

Assuming $\text{SU}_f(3)$ flavor symmetry, substituting Eq. (27) into Eq. (26) gives

$$\omega_5^{fg}(P) = \delta^{fg} \frac{1}{P^2 + m_H^2} Z_m^{-2} r_H^2 + \dots \quad (28)$$

(the ellipsis denotes terms regular in the pole's neighborhood). The renormalizable correlation function in Eq. (25) is the Fourier transform of Eq. (28), and using this fact plus the definitions in Eqs. (12) and (23) it is evident that the large (Euclidean) x^2 behavior of the product

$$m_{\text{bm}}^2 \Delta_5(x) \quad (29)$$

is a direct measure of the renormalization-group invariant

$$[m(\zeta) r_H^{(\zeta)}]^2 \quad (30)$$

that appears in Eq. (18). (This observation merely adapts the technique for extracting masses in numerical simulations of lattice-QCD.) Hence the correlator in Eq. (25) provides a means of estimating the OPE condensate in lattice simulations [21], one whose ultraviolet behavior ensures a well-defined and calculable evolution under the renormalization group for any value of the current-quark mass. [f_π can similarly be extracted from the axial-vector correlator analogous to Eq. (25).] The model of Ref. [22] yields a meson mass trajectory via Eq. (18) that provides a qualitative and quantitative understanding of recent quenched lattice simulations [20].

III. BANKS-CASHER RELATION

A. Continuum analysis

It is readily apparent that Eq. (6) is meaningless as written: dimensional counting reveals that the rhs has mass-dimension three and since λ will at some point be greater than any relevant internal scale, the integral must diverge as Λ^2 , where Λ is the regularizing mass scale.

To learn more, consider the trace of the unrenormalized massive dressed-quark propagator:

$$\tilde{\sigma}(m) := N_c \text{tr}_D \int_p^\Lambda \tilde{S}_m(p), \quad (31)$$

evaluated at a fixed value of the regularization scale, Λ . This Schwinger function can be identified with the left-hand side of Eq. (6). Furthermore, assume that $\tilde{\sigma}(m)$ has a spectral representation, since this is the essence of the Banks-Casher relation:

$$\tilde{\sigma}(m) := 2m \int_0^\Lambda d\lambda \frac{\tilde{\rho}(\lambda)}{\lambda^2 + m^2}, \quad (32)$$

where $m = m^{\text{bm}}(\Lambda)$. Equation (32) entails

$$\tilde{\rho}(\lambda) = \frac{1}{2\pi} \lim_{\eta \rightarrow 0^+} [\tilde{\sigma}(i\lambda + \eta) - \tilde{\sigma}(i\lambda - \eta)]. \quad (33)$$

The content and meaning of this sequence of equations is well illustrated by inserting the free quark propagator in Eq. (31). The integral thus obtained is readily evaluated using dimensional regularization:

$$\tilde{\sigma}_{\text{free}}(m) = \frac{N_c}{4\pi^2} m^3 \left[\ln \frac{m^2}{\zeta^2} + \frac{1}{\varepsilon} + \gamma - \ln 4\pi \right]. \quad (34)$$

With Eq. (33) the regularization dependent terms cancel and one obtains

$$\tilde{\rho}(\lambda) = \frac{N_c}{4\pi^2} \lambda^3. \quad (35)$$

The one-loop contribution to $\tilde{\rho}(\lambda)$ has been evaluated using the same procedure [23]. It is also proportional to λ^3 and arises from the $m^3 \ln m^2/\zeta^2$ terms in $\tilde{\sigma}(m)$. In fact, every term obtainable in perturbation theory is proportional to λ^3 , for precisely the same reason that each term in the perturbative expression for the scalar part of the quark propagator is proportional to m , see Eq. (24). Hence, at every order in perturbation theory,

$$\tilde{\rho}(\lambda=0) = 0 \quad (36)$$

and $\langle 0 | \bar{q}q | 0 \rangle = 0$. A nonzero value of $\rho(0)$ is plainly an essentially nonperturbative effect.

A precise analysis requires that attention be paid to renormalization. Consider then the gauge-parameter-independent trace of the renormalized quark propagator evaluated at a fixed value of the regularization scale:

$$\sigma(m, \zeta) := - \lim_{x \rightarrow 0} \langle \bar{q}(x) q(0) \rangle = Z_4(\zeta, \Lambda) N_c \text{tr}_D \int_p^\Lambda S_m(p; \zeta), \quad (37)$$

where the argument remains $m = m^{\text{bm}}(\Lambda)$, which is permitted because $m^{\text{bm}}(\Lambda)$ is proportional to the renormalization-point-independent current-quark mass. The renormalization constant Z_4 vanishes logarithmically with increasing Λ and hence one still has $\sigma(m) \sim \Lambda^2 m^{\text{bm}}(\Lambda)$. However, using Eq. (22) it is clear that for any finite but large value of Λ and tolerance δ , it is always possible to find $m_\delta^{\text{bm}}(\Lambda)$ such that

$$\sigma(m, \zeta) + \langle \bar{q}q \rangle_\zeta^0 < \delta, \forall m^{\text{bm}} < m_\delta^{\text{bm}}. \quad (38)$$

This is true in QCD. It can be illustrated using the DSE model of Ref. [2], which preserves the one-loop renormalization group properties of QCD. In Fig. 1 we plot $\sigma(m, \zeta)$, evaluated using a hard cutoff Λ on the integral in Eq. (37), calculated with the massive dressed-quark propagators obtained by solving the gap equation as described in the Appendix. Since Eq. (38) specifies the domain on which the value of $\sigma(m, \zeta)$ is determined by nonperturbative effects, one anticipates

$$m_\delta^{\text{bm}}(\Lambda) \approx - \langle \bar{q}q \rangle_\zeta^0 / \Lambda^2 \sim 10^{-9} \quad (39)$$

for $\Lambda = 2.0$ TeV in QCD where $|\langle \bar{q}q \rangle_\zeta^0| \sim \Lambda_{\text{QCD}}^3$, an estimate confirmed in Fig. 1.

The dotted line in Fig. 1 is

$$\begin{aligned} \sigma(m, \zeta) = & - \langle \bar{q}q \rangle_\zeta^0 \frac{2}{\pi} \arctan \frac{\Lambda}{m} + Z_4(\zeta, \Lambda) \frac{N_c}{4\pi^2} \\ & \times m [\Lambda^2 - m^2 \ln(1 + \Lambda^2/m^2)]. \end{aligned} \quad (40)$$

(We used the one-loop formula: $Z_4(\zeta, \Lambda) = [\alpha(\Lambda)/\alpha(\zeta)]^{\gamma_m}$, for the numerical comparison.) The difference between Eq.

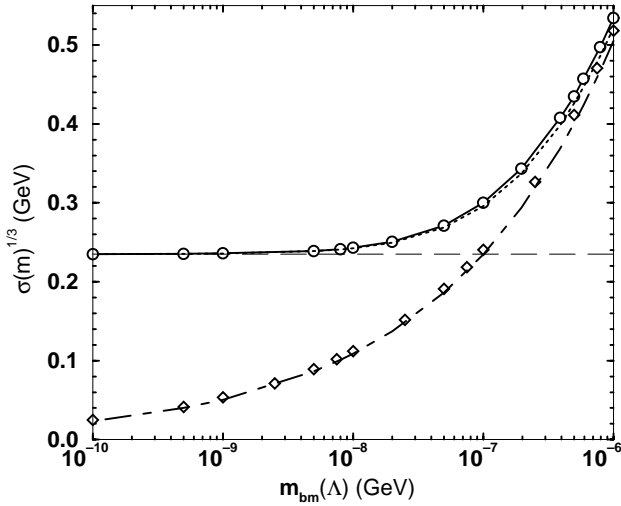


FIG. 1. Circles/solid line: $\sigma(m)^{1/3}$ in Eq. (37) as a function of the current-quark bare mass, evaluated using the dressed-quark propagator obtained in the model of Ref. [2]; dashed line: the model's value of $(-\langle\bar{q}q\rangle_{\xi=1\text{ GeV}}^0) = (0.24\text{ GeV})^3$; and dotted line: Eq. (40). Diamonds: $\sigma(m)^{1/3}$ evaluated in a nonconfining version of the model; dot-dashed line: Eq. (40) with $\langle\bar{q}q\rangle^0 \equiv 0$.

(40) and the curve is of $O[\alpha(\Lambda)m(\Lambda)\Lambda^2]$ because the DSE model incorporates QCD's one-loop behavior. In Fig. 1 we also plot $\sigma(m, \zeta)$ obtained in the absence of confinement, in which case [24] $\langle\bar{q}q\rangle^0 \equiv 0$, as is evident.

The discussion establishes that $\sigma(m, \zeta)$ has a regular chiral limit in QCD and is a monotonically increasing convex-up function. It follows that $\sigma(m, \zeta)$ has a spectral representation:

$$\sigma(m, \zeta) = 2m \int_0^\Lambda \frac{\rho(\lambda)}{\lambda^2 + m^2}. \quad (41)$$

This lays the vital plank in a veracious connection between the condensates in Eqs. (1) and (8). On the domain specified by Eq. (39), the behavior of $\sigma(m, \zeta)$ in Eq. (37) is given by Eq. (40), which yields, via Eq. (33),

$$\pi\rho(\lambda) = -\langle\bar{q}q\rangle_\xi^0 + Z_4(\zeta, \Lambda) \frac{N_c}{4\pi} \lambda^3 + \dots, \quad (42)$$

where the ellipsis denotes contributions from the higher-order terms implicit in Eq. (40).

B. Comparison with a lattice-QCD simulation

In Fig. 2 we plot the spectral density of the staggered Dirac operator in quenched $SU(3)$ gauge theory calculated with 3000 configurations obtained on a $V=4^4$ lattice, in the vicinity of the deconfining phase transition at $\beta \gtrsim 5.6$. Details of the simulation are given in Ref. [12]. Dimensioned quantities are measured in units of $1/a$, where a is the lattice spacing, and it is $\rho(\lambda)/V$ that should be compared with the continuum spectral density.

While the effect of finite lattice volume is apparent in Fig. 2 for $\lambda a \gtrsim 0.1$, the behavior at small λa is qualitatively in

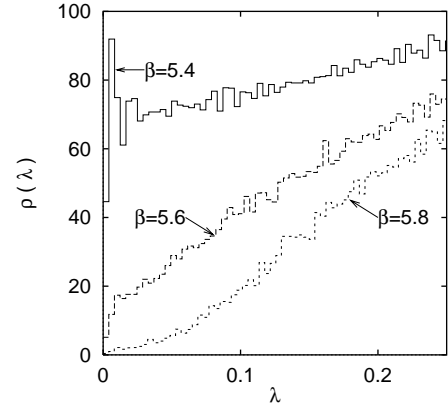


FIG. 2. Spectral density of the staggered Dirac operator in quenched $SU(3)$ gauge theory calculated on a 4^4 lattice. (Measured in units of the lattice spacing.) The deconfinement transition takes place at $\beta \gtrsim 5.6$.

agreement with Eq. (42) and Fig. 1: a nonzero OPE condensate dominates the Dirac spectrum in the confined domain; and it vanishes in the deconfined domain whereupon $\rho(0) = 0$ and the perturbative evolution, Eq. (35), is manifest.

To be more quantitative, we note that at $\beta = 5.4$, $\rho(0)a^3 \approx 70$, so that

$$\pi\rho(0)a^3/V \approx (0.95)^3. \quad (43)$$

The value of the lattice spacing was not measured in Ref. [12] but one can, nevertheless, assess the scale of Eq. (43) by supposing $a \sim 0.3\text{ fm} \sim 0.3/\Lambda_{\text{QCD}}$, a value typical of small couplings, β , wherewith the rhs is $\sim (3\Lambda_{\text{QCD}})^3$. This is too large but not unreasonable given the parameters of the simulation, its errors, and the systematic uncertainties in our estimate. One can also fit the lattice data at $\beta = 5.8$, whereby one finds $\rho(\lambda) \propto \lambda^3$ on $\lambda < 0.1$ but with a proportionality constant larger than that anticipated from perturbation theory viz., Eq. (42). Some mismatch is to be expected because at $\beta = 5.8$ one has only just entered the deconfined domain and close to the transition boundary nonperturbative effects are still material, as seen, e.g., in the heavy-quark potential and equation of state [25]. It is a modern challenge to determine those gauge couplings and lattice parameters for which the data are quantitatively consistent with Eq. (42).

IV. EPILOGUE

We verified that the gauge-invariant trace of the massive dressed-quark propagator possesses a spectral representation when considered as a function of the current-quark mass. This is key to establishing that the OPE condensate, which sets the ultraviolet scale for the momentum dependence of the trace of the dressed-quark propagator, does indeed measure the density of far-infrared eigenvalues of the gauge-averaged massless Dirac operator, in the manner of the Banks-Casher relation. This relation is intuitively appealing because a measurable accumulation of eigenvalues of the massless Dirac operator at zero virtuality expresses a mass gap in its spectrum.

In practice, there are three main parameters in a simulation of lattice-QCD: the lattice volume, characterized by a length L ; the lattice spacing a ; and the current-quark mass m . So long as the lattice size is large compared with the current-quark's Compton wavelength, viz., $L \gg 1/m$, then dynamical chiral symmetry breaking can be expressed in the simulation. Supposing that to be the case then, as we have explicated, so long as the lattice spacing is small compared with the current-quark's Compton wavelength, i.e., $a \ll 1/m \ll L$,

$$\pi\rho(0) \approx -\langle \bar{q}q \rangle_{1/a}^0, \quad (44)$$

where the rhs is the scale-dependent OPE condensate [$\zeta = \Lambda = 1/a$ in Eq. (42)].

In our continuum analysis we found that one requires $am \lesssim (a\Lambda_{\text{QCD}})^3$ if $\rho(\lambda=0)$ is to provide a veracious estimate of the OPE condensate. The residue at the lowest-mass pole in the flavor-nonsinglet pseudoscalar vacuum polarization provides a measure of the OPE condensate that is accurate for larger current-quark masses.

ACKNOWLEDGMENTS

We benefited from interactions with M. A. Pichowsky and P. C. Tandy. This work was supported by Deutsche Forschungsgemeinschaft, under Contract No. Ro 1146/3-1; the Department of Energy, Nuclear Physics Division, under Contract No. W-31-109-ENG-38; the National Science Foundation under Grant No. INT-0129236; and benefited from the resources of the National Energy Research Scientific Computing Center.

APPENDIX: MODEL GAP EQUATION

The gap equation's kernel is built from a product of the dressed-gluon propagator and dressed-quark-gluon vertex. It can be calculated in perturbation theory but that is inadequate for the study of intrinsically nonperturbative phenomena. To make model-independent statements about DCSB, one must employ an alternative systematic and chiral symmetry preserving truncation scheme.

The leading order term in one such scheme [26] is the renormalization-group-improved rainbow truncation of the gap equation ($Q = p - q$),

$$S(p)^{-1} = Z_2(i\gamma \cdot p + m^{\text{bm}}) + \int_q^\Lambda \mathcal{G}(Q^2) D_{\mu\nu}^{\text{free}}(Q) \frac{\lambda^a}{2} \gamma_\mu S(q) \frac{\lambda^a}{2} \gamma_\nu. \quad (A1)$$

The ultraviolet ($Q^2 \gtrsim 1 \text{ GeV}^2$) behavior of $\mathcal{G}(Q^2)$ in Eq. (A1) is fixed by the known behavior of the quark-antiquark scattering kernel [2]. The form of that kernel on the infrared domain is currently unknown and a model is employed to complete the specification of the kernel. An efficacious form is [2]

$$\frac{\mathcal{G}(Q^2)}{Q^2} = 8\pi^4 D \delta^4(k) + \frac{4\pi^2}{\omega^6} D Q^2 e^{-Q^2/\omega^2} + 4\pi \frac{\gamma_m \pi}{\frac{1}{2} \ln[\tau + (1 + Q^2/\Lambda_{\text{QCD}}^2)^2]} \mathcal{F}(Q^2), \quad (A2)$$

where, $\mathcal{F}(Q^2) = \{1 - \exp(-Q^2/[4m_t^2])\}/Q^2$, $m_t = 0.5 \text{ GeV}$; $\tau = e^2 - 1$; $\gamma_m = 12/(33 - 2N_f)$, $N_f = 4$; and $\Lambda_{\text{QCD}} = \Lambda_{\overline{\text{MS}}}^{(4)} = 0.234 \text{ GeV}$. The true parameters in Eq. (A2) are D and ω ; however, they are not independent: in fitting, a change in one is compensated by altering the other, with fitted observables changing little along a trajectory $\omega D = (0.6 \text{ GeV})^3$. Herein we used

$$D = (0.884 \text{ GeV})^2, \quad \omega = 0.3 \text{ GeV}. \quad (A3)$$

A nonconfining model is obtained with $D = 0$.

Equation (A1) is readily solved for the dressed-quark propagator, with the renormalization constants fixed via Eq. (11). That solution provides the elements used in the illustration of Sec. III.

-
- [1] K.D. Lane, Phys. Rev. D **10**, 2605 (1974); H.D. Politzer, Nucl. Phys. **B117**, 397 (1976).
 [2] P. Maris and C.D. Roberts, Phys. Rev. C **56**, 3369 (1997).
 [3] C.D. Roberts and A.G. Williams, Prog. Part. Nucl. Phys. **33**, 477 (1994).
 [4] P.O. Bowman, U.M. Heller, and A.G. Williams, Phys. Rev. D **66**, 014505 (2002).
 [5] J.B. Zhang, F.D.R. Bonnet, P.O. Bowman, D.B. Leinweber, and A.G. Williams, hep-lat/0208037.
 [6] P. Maris, A. Raya, C.D. Roberts, and S.M. Schmidt, nucl-th/0208071.
 [7] In our Euclidean metric: $\{\gamma_\mu, \gamma_\nu\} = 2\delta_{\mu\nu}$; $\gamma_\mu^\dagger = \gamma_\mu$; and $a \cdot b = \sum_{i=1}^4 a_i b_i$.
 [8] Zero modes were neglected in deriving Eq. (4), which is justified under broad conditions, as discussed in detail in Ref. [9]:

- if the condensate is large, the number of zero modes per unit volume tends to zero in the limit $V \rightarrow \infty$ and they contribute a fraction of the total condensate that vanishes as $1/\sqrt{V}$.
 [9] H. Leutwyler and A. Smilga, Phys. Rev. D **46**, 5607 (1992).
 [10] T. Banks and A. Casher, Nucl. Phys. **B169**, 103 (1980).
 [11] E. Marinari, G. Parisi, and C. Rebbi, Phys. Rev. Lett. **47**, 1795 (1981).
 [12] E. Bittner, H. Markum, and R. Pullirsch, Nucl. Phys. (Proc. Suppl.) **96A**, 189 (2001).
 [13] E. Bittner, M.P. Lombardo, H. Markum, and R. Pullirsch, Nucl. Phys. (Proc. Suppl.) **94A**, 445 (2001).
 [14] T. Bielefeld, S. Hands, J.D. Stack, and R.J. Wensley, Phys. Lett. B **416**, 150 (1998).
 [15] J.J. Verbaarschot, Phys. Rev. Lett. **72**, 2531 (1994); J.J. Verbaarschot and T. Wettig, Annu. Rev. Nucl. Part. Sci. **50**, 343 (2000).

- [16] M.E. Berbenni-Bitsch, S. Meyer, A. Schäfer, J.J. Verbaarschot, and T. Wettig, Phys. Rev. Lett. **80**, 1146 (1998); M. Göckeler, H. Hehl, P.E. Rakow, A. Schäfer, and T. Wettig, Phys. Rev. D **59**, 094503 (1999); R.G. Edwards, U.M. Heller, J.E. Kiskis, and R. Narayanan, Phys. Rev. Lett. **82**, 4188 (1999); B.A. Berg, H. Markum, R. Pullirsch, and T. Wettig, Phys. Rev. D **63**, 014504 (2001); P.H. Damgaard, U.M. Heller, R. Niclasen, and K. Rummukainen, Phys. Lett. B **495**, 263 (2000); B.A. Berg, U.M. Heller, H. Markum, R. Pullirsch, and W. Sakuler, *ibid.* **514**, 97 (2001).
- [17] P. Maris, C.D. Roberts, and P.C. Tandy, Phys. Lett. B **420**, 267 (1998).
- [18] C.D. Roberts and S.M. Schmidt, Prog. Part. Nucl. Phys. **45**, S1 (2000); R. Alkofer and L.v. Smekal, Phys. Rep. **353**, 281 (2001); P. Maris and C.D. Roberts, nucl-th/0301049.
- [19] M.A. Ivanov, Yu.L. Kalinovsky, and C.D. Roberts, Phys. Rev. D **60**, 034018 (1999).
- [20] C.D. Roberts, Nucl. Phys. (Proc. Suppl.) **108A**, 227 (2002).
- [21] P. Hernandez, K. Jansen, L. Lellouch, and H. Wittig, J. High Energy Phys. **0107**, 018 (2001); A. Duncan, S. Pernice, and J. Yoo, Phys. Rev. D **65**, 094509 (2002).
- [22] P. Maris and P.C. Tandy, Phys. Rev. C **60**, 055214 (1999).
- [23] K. Zyablyuk, J. High Energy Phys. **06**, 025 (2000).
- [24] F.T. Hawes, C.D. Roberts, and A.G. Williams, Phys. Rev. D **49**, 4683 (1994); A. Bender, D. Blaschke, Yu.L. Kalinovsky, and C.D. Roberts, Phys. Rev. Lett. **77**, 3724 (1996); F.T. Hawes, P. Maris, and C.D. Roberts, Phys. Lett. B **440**, 353 (1998).
- [25] E. Laermann, Fiz. Élem. Chastits At. Yadra **30**, 720 (1999) [Phys. Part. Nucl. **30**, 304 (1999)].
- [26] A. Bender, C.D. Roberts, and L.v. Smekal, Phys. Lett. B **380**, 7 (1996); A. Bender, W. Detmold, A.W. Thomas, and C.D. Roberts, Phys. Rev. C **65**, 065203 (2002).